

# Improving the accuracy of mass reconstructions from weak lensing: local shear measurements

Marco Lombardi and Giuseppe Bertin

Scuola Normale Superiore, Piazza dei Cavalieri 7, I 56126 Pisa, Italy

[the date of receipt and acceptance should be inserted later]

**Abstract.** Different options can be used in order to measure the shear from observations in the context of weak lensing. Here we introduce new methods where the isotropy assumption for the distribution of the source galaxies is implemented directly on the observed quadrupole moments. A quantitative analysis of the error associated with the finite number of source galaxies and with their ellipticity distribution is provided, applicable even when the shear is not weak. Monte Carlo simulations based on a realistic sample of source galaxies show that our procedure generally leads to errors  $\approx 30\%$  smaller than those associated with the standard method of Kaiser and Squires (1993).

**Key words:** gravitational lensing – dark matter – galaxies: clustering

## 1. Introduction

One of the most interesting applications of gravitational lenses arises in the context of weak distortions of far sources (e.g., see Tyson *et al.* 1984, Webster 1985). The presence of a gravitational lens (e.g., an intervening cluster of galaxies) breaks the symmetry of the image of an isotropic population of extended sources, with the lensed objects preferentially oriented in the tangential direction with respect to the center of the lens. This effect is usually quantified in terms of the *shear* introduced by the lens. In turn, the shear field measured from the observed anisotropy and stretching in a field of distant objects can be used to infer the two-dimensional (projected) mass distribution of the lens (see Kaiser and Squires 1993; Kaiser *et al.* 1995).

At present these concepts have found application in two different classes of lenses, i.e. galaxies and clusters. The work on galaxies has been performed via a statistical investigation of a suitable ensemble (Griffiths *et al.* 1996, Brainerd *et al.* 1996), due to the limited number of

background sources generally associated with an individual galaxy. Relatively nearby clusters, instead, are ideal candidates for direct weak lens analyses (e.g., Kneib *et al.* 1996; for a review, see Kneib and Soucail 1995; see also Gould and Villumsen 1994); these studies are especially important in relation to the problem of dark matter on the megaparsec scale, with significant cosmological implications.

In this paper we focus on the measurement of shear from observations, as a key step in the process of estimating the mass of a cluster of galaxies from weak gravitational lensing. We discuss the possible merits of alternative options in handling a given set of data under the same conditions for the population of background sources. Different methods may introduce different forms of bias, depending on whether the data are degraded by seeing or by other effects. In this article we give special attention to one aspect of the problem which is largely independent of the specific characteristics of the observations involved. This important factor in determining the size of the *error* in the shear measurement is the ellipticity distribution of the source galaxies. In Sect. 2, with a short discussion of the “standard” method of Kaiser and Squires (1993), we provide an expression for the expected error in a shear measurement as a function of the ellipticity distribution of the sources. This result is not restricted to a weak shear analysis. Then, in Sect. 3, we introduce a different method, directly based on the observed quadrupole moments, which retains information not only on the shape of the observed objects, but also on their angular size, and we carry out the related error analysis. The method is shown to implement correctly the hypothesis of a random orientation of the sources; it is also shown to be fully equivalent to the “standard” method if applied to a population of nearly round source objects. The method is then generalized and further improved by introducing suitable weight functions to optimize the inversion procedure. In Sect. 4 we describe the results of a wide set of Monte Carlo simulations applied to realistic distributions of ellipticities for the source galaxies. These show that the new method

Send offprint requests to: M. Lombardi

proposed in this paper can be significantly more accurate than the standard method in determining the shear from the data. The simulations also confirm that the applicability of the method and the conclusions on its accuracy do not depend on the strength of the lens in a relatively wide parameter range. The implications on the accuracy of mass measurements are discussed in Sect. 5.

## 2. The isotropy hypothesis and the “standard” method

### 2.1. Notation

Following standard notation with minor modifications (see Schneider et al. 1992), let  $\theta^s$  be the unlensed position of a point source and  $\theta$  the position of the corresponding observed image. We will generally refer to a Cartesian representation of the *angle* vectors, so that  $\theta = (\theta_1, \theta_2)$ . The deflection angle  $\beta$  is defined through the relation

$$\theta^s = \theta - \beta(\theta). \quad (1)$$

For a single thin lens we can define  $D_{os}$ ,  $D_{ds}$ , and  $D_{od}$  as the distances between the observer (o), the lens or deflector (d), and the source (s). In this case the deflection angle can be expressed as a function of the dimensionless mass distribution  $\sigma(\theta) = \Sigma(\theta)/\Sigma_c$ , where  $\Sigma(\theta)$  is the projected mass distribution of the deflector and  $\Sigma_c = c^2 D_{os}/(4\pi G D_{ds} D_{od})$  is the critical density; it is given by

$$\beta(\theta) = \frac{1}{\pi} \int \frac{\sigma(\theta')(\theta - \theta')}{\|\theta - \theta'\|^2} d^2\theta'. \quad (2)$$

Thus for a small extended source in the vicinity of  $\theta = \theta_0$  we have  $\theta^s \simeq \theta^s(\theta_0) + J(\theta_0)(\theta - \theta_0)$ , with

$$\begin{aligned} J(\theta) &= \left( \frac{\partial \theta^s}{\partial \theta} \right) \\ &= \begin{pmatrix} 1 - \sigma(\theta) + \gamma_1(\theta) & \gamma_2(\theta) \\ \gamma_2(\theta) & 1 - \sigma(\theta) - \gamma_1(\theta) \end{pmatrix} \\ &= (1 - \sigma(\theta)) \begin{pmatrix} 1 + g_1(\theta) & g_2(\theta) \\ g_2(\theta) & 1 - g_1(\theta) \end{pmatrix}. \end{aligned} \quad (3)$$

The complex quantity  $\gamma = \gamma_1 + i\gamma_2$  is called shear because it is responsible for the distortion of the image. The reduced shear parameter is defined as  $g = g_1 + ig_2 = \gamma/(1 - \sigma)$  and is the quantity actually derived from the observations; note that for a weak lens  $g \simeq \gamma$ .

From the surface brightness distribution  $I(\theta)$  of an extended object we can define the total luminosity  $I$ , the position vector of the center of the image  $\mathbf{d}$ , and the image quadrupole  $Q_{ij}$  as

$$I = \int I(\theta) d^2\theta, \quad (4)$$

$$\mathbf{d} = \frac{1}{I} \int \theta I(\theta) d^2\theta, \quad (5)$$

$$Q_{ij} = \frac{1}{I} \int (\theta_i - d_i)(\theta_j - d_j) I(\theta) d^2\theta. \quad (6)$$

The quadrupole  $Q_{ij}$  gives information on angular size, shape, and orientation of the observed galaxy. If we are not interested in the image size, we may refer to the (complex) ellipticity  $\chi$ :

$$\chi = \chi_1 + i\chi_2 = \frac{Q_{11} - Q_{22} + 2iQ_{12}}{Q_{11} + Q_{22}} = \chi(Q). \quad (7)$$

The modulus of  $\chi$  is related to the shape ( $|\chi| = 0$  for a circular object) while its argument is twice the image orientation angle (angle between the  $\theta_1$  axis and the galaxy major axis).

Similar definitions can be given for the unlensed source, with  $I(\theta)$  replaced by the source luminosity flux  $I^s(\theta^s)$ . For a small object a simple relation holds between the observed and the source quadrupole moment:

$$Q^s = JQJ, \quad (8)$$

where we have used the symmetry of  $J$ . The corresponding relation between  $\chi$  and  $\chi^s$  is (here an asterisk denotes complex conjugation)

$$\chi^s = \frac{\chi + 2g + \chi^*g^2}{1 + 2\text{Re}(\chi^*g) + |g|^2} = \chi^s(\chi, g). \quad (9)$$

Thus  $\chi^s$  is a function of  $\chi$  and  $g$  only.

### 2.2. The standard method (X method)

The local value of  $g$  can be derived from the observation of a large number  $N$  of galaxies in a small patch of the sky. For the purpose, it is usually assumed that the population of source objects is *isotropic*, i.e. that the source galaxies have random orientations. The area of the sky under consideration must be small so that the Jacobian matrix can be considered to be approximately constant, i.e. the same for all the galaxies observed in the area. The source galaxies are taken to have  $D_{os}/D_{ds} \simeq \text{constant}$ , which is a reasonable assumption for far away sources lensed by a nearby cluster.

The standard method (X method) of Kaiser and Squires (1993) implements the isotropy hypothesis by arguing that the quantity

$$\tilde{\chi}^s = \frac{1}{N} \sum_{n=1}^N \chi^s(\chi^{(n)}, g) \quad (10)$$

vanishes approximately. For a given set of data  $\{\chi^{(n)}\}$ , with  $n = 1, \dots, N$ , the condition

$$\tilde{\chi}^s = 0 \quad (11)$$

is used to determine the reduced shear parameter  $g$ . In terms of the probability distribution for the *source* ellipticities  $p(\chi^s)$ , the isotropy hypothesis states that  $p(\chi^s) = p(|\chi^s|)$ . Thus we have  $\langle \chi^s \rangle = 0$ , with a scalar covariance matrix  $\langle \chi_i^s \chi_j^s \rangle = c\delta_{ij}$ . [Here the indices refer to the representation of the complex shear as  $\chi = \chi_1 + i\chi_2$ .] Given

the range of values for  $|\chi|$ , we must have  $c \leq 1/2$ . Then the central limit theorem ensures that the variable  $\tilde{\chi}^s$  of Eq. (10), calculated for  $N$  galaxies, must converge to a Gaussian with mean 0 and covariance matrix  $(c/N)\delta_{ij}$  in the limit  $N \gg 1$ .

### 2.3. Error analysis for the standard method

Here we consider the simple case of a *sharp* distribution of source ellipticities, when the population of objects is basically made of nearly round source galaxies. We then assume that the probability distribution  $p$  is characterized by  $c \ll 1$ . For such distributions, the condition  $\tilde{\chi}^s = 0$  is shown to give a correct determination of the reduced shear parameter  $g$  (see Appendix A). If we perform a measurement for a lens with true reduced shear equal to  $g_0$ , then the expected statistics for  $g$  has mean and covariance given by

$$\langle g \rangle = g_0, \quad (12)$$

$$\text{Cov}_{ij}(g) = \frac{c(1 - |g_0|^2)^2}{4N} \delta_{ij}. \quad (13)$$

Here and in the following, by  $\text{Cov}_{ij}(X) = \langle (X_i - \bar{X}_i)(X_j - \bar{X}_j) \rangle$  we denote the covariance matrix for the random variable  $X$  with mean  $\bar{X} = \langle X \rangle$ . The expected error,  $\sigma_g = |1 - |g_0|^2| \sqrt{c/4N}$ , is the same on  $g_1$  and on  $g_2$ .

The error depends on the source distribution via the parameter  $c$  and shows that the method can lead to an accurate measurement of  $g$  provided  $N$  is sufficiently large. The error analysis in the general case of a broad distribution ( $c \lesssim 1/2$ ) is much more difficult. However, if we naively extrapolate the conclusions obtained for sharp distributions, the largest error on  $g_1$  and on  $g_2$  should be  $|1 - |g_0|^2|/\sqrt{8N}$ . In the opposite limit, when  $c = 0$ , the error vanishes. In fact, when  $c = 0$  all galaxies are circular. In this situation the value of  $g_0$  can be derived simply by observing the shape of a single galaxy, and thus the error on  $g$  is zero.

The dependence of the error on  $g_0$  is quite interesting. For  $|g_0| < 1$  the error decreases with increasing  $|g_0|$ , and it vanishes when  $|g_0| = 1$ . This happens because for  $|g_0| = 1$  the lens is singular, since  $\det J \sim (1 - |g_0|^2) = 0$ , which means that all galaxies are seen as thin segments, with  $|\chi| = 1$ . If the source population is made of nearly round galaxies, by observing even a single galaxy with very high ellipticity, we can immediately infer that  $|g_0| \simeq 1$ ; of course the argument of  $g_0$  is given by the orientation of the galaxy. The behavior of the error for  $|g_0| > 1$  is explained in terms of the  $g_0 \mapsto 1/g_0^*$  local invariance (Schneider & Seitz 1995a, b). Thus it should be possible to infer the error for a value of  $g_0$  with modulus  $|g_0| > 1$  from the error for  $g_0' = 1/g_0^*$ . In fact (see Appendix A), the *relative* errors for  $g_0$  and  $g_0'$  are the same.

## 3. Alternative methods based on the observed average quadrupole

### 3.1. Simple quadrupoles ( $Q$ method)

We now introduce a new method based on the observed quadrupole moments rather than on ellipticities ( $Q$  method). In order to implement the isotropy assumption we replace condition (11) by

$$\chi^s \left( \frac{1}{N} \sum_{n=1}^N Q^{(n)}, g \right) = 0. \quad (14)$$

Note that here the average is performed *inside the parentheses*, i.e. on the observed quadrupoles. Then it is argued that the average quadrupole is traced back to a *circular source*. The method is thus similar to the one used by Bonnet & Mellier (1995), but with an important difference in that we refer to an average on quadrupole moments, which gives different weights to galaxies with different angular sizes.

To see why Eq. (14) holds, we define the probability distribution for the *source* quadrupole moments  $p_Q(Q^s)$ . Since the quadrupole matrix  $Q_{ij}^s$  is symmetric,  $p_Q(Q^s)$  is a function of three real quantities  $\mathcal{Q}_1^s = Q_{11}^s$ ,  $\mathcal{Q}_2^s = Q_{12}^s = Q_{21}^s$ , and  $\mathcal{Q}_3^s = Q_{22}^s$ . The isotropy hypothesis states that the probability distribution  $p_Q$  is independent of the orientation of the galaxy, so that  $\langle Q^s \rangle = M \text{Id}$ , with  $\text{Id}$  the  $2 \times 2$  identity matrix. Furthermore, isotropy requires the covariance matrix of  $\mathcal{Q}^s$  to be of the form

$$\text{Cov}_{kl}(\mathcal{Q}^s) = \begin{pmatrix} a+b & 0 & a-b \\ 0 & b & 0 \\ a-b & 0 & a+b \end{pmatrix}. \quad (15)$$

As the covariance matrix is positive definite, we must have  $a, b \geq 0$ . Here the two indices  $k$  and  $l$  run on the three independent components of  $\mathcal{Q}^s$ . It is possible to show that  $b$  is related to the constant  $c$  defined earlier in Sect. 2.2, as  $c = b/M^2$ , while  $a$  is the variance of  $Q_{11}^s + Q_{22}^s$ , the dimension of the galaxy.

If we have a large number  $N$  of galaxies with quadrupole moments  $\{Q^{(n)}\}$ , with  $n = 1, \dots, N$ , we can write

$$J \left( \frac{1}{N} \sum_{n=1}^N Q^{(n)} \right) J = \frac{1}{N} \sum_{n=1}^N Q^{s(n)} \simeq M \text{Id}, \quad (16)$$

where the approximate sign is used because  $N$  is finite. Let us now calculate the ellipticity  $\chi$  for both sides of this equation by applying the definition given by Eq. (7)

$$\chi \left( J \left( \frac{1}{N} \sum_{n=1}^N Q^{(n)} \right) J \right) \simeq \chi(M \text{Id}) = 0. \quad (17)$$

Equation (17) is the result stated in Eq. (14), because  $\chi(JQJ) = \chi^s(Q, g)$ .

The reduced shear  $g$  calculated through Eq. (14) is a good estimate of the true reduced shear  $g_0$ . In Appendix A

we show that in the case of sharp distributions the quantity  $g$  has mean and covariance matrix given by

$$\langle g \rangle = g_0, \quad (18)$$

$$\text{Cov}_{ij}(g) = \frac{c(1 - |g_0|^2)^2}{4N} \delta_{ij}. \quad (19)$$

Note that these expressions are exactly the same as for the standard method. This apparently surprising result can be traced to the decoupling of size and ellipticity distributions for quasi-circular sources. This property is shown directly by Eq. (15), where  $\text{Cov}(Q^s)$  is found to depend on two quantities,  $a$  being related to the size distribution and  $b$  being related to the ellipticity.

### 3.2. Weighted quadrupoles (W method)

The simple quadrupole method described in Sect. 3.1 is based on the isotropy requirement  $\langle Q^s \rangle = M \text{Id}$ , which leads to Eq. (16) and thus justifies the use of Eq. (14). Since the analysis has shown that  $g$  is determined more accurately when the ellipticities involved are smaller, we may argue that a generalization where a *penalty* is assigned to galaxies with large  $|\chi^s|$  should be able to improve the method. Thus we introduce a weight function  $W(Q^s) > 0$  with the following requirements:

1.  $W$  is invariant under rotation (consistent with the isotropy of  $p_Q(Q^s)$ ).
2. If  $k$  is a constant multiplying factor,  $W(kQ^s) = f(k)W(Q^s)$  (consistent with the fact that the analysis of the data is able to constrain  $J$  only up to a multiplying factor  $(1 - \sigma)$ ).
3.  $W(Q^s)$  penalizes objects with large  $|\chi^s|$ .

Under these conditions we may now consider as the starting point the relation  $\langle Q^s W(Q^s) \rangle = M_W \text{Id}$ , with  $M_W$  a positive number dependent on  $W$ , which holds because of the isotropy assumption. Then, following the argument that has led to Eq. (17), we find

$$\chi \left( J \left( \frac{1}{N} \sum_{n=1}^N Q^{(n)} W(JQ^{(n)}J) \right) J \right) \simeq \chi(M_W \text{Id}) = 0, \quad (20)$$

which indicates that we could replace Eq. (14) by

$$\chi^s \left( \frac{1}{N} \sum_{n=1}^N Q^{(n)} W(JQ^{(n)}J), g \right) = 0. \quad (21)$$

In this method based on weighted quadrupoles (W method) one has to proceed by iteration, because the quadrupoles  $JQ^{(n)}J = Q^{s(n)}$  that appear in the weight functions are not given directly by the data but must be guessed first in order to start the iteration procedure. Several alternatives have been considered. One possibility is to take the result of the method described in Sect. 3.1 as

the initial seed for the iteration. Another reasonable choice is to take the natural approximation of the weak lensing limit, i.e.  $g \simeq -(1/2N) \sum_n \chi^{(n)}$ , or the estimate obtained from  $g/(1 + |g|^2) = -(1/2N) \sum_n \chi^{(n)}$  applicable beyond the weak lensing limit (see Appendix A).

As far as the choice of the weight functions is concerned, we have found that a logarithmic dependence

$$W(Q^s) = -\ln(|\chi^s|). \quad (22)$$

is simple and suitable for the purpose.

Note that a similar weight function could be introduced also for the standard X method, but the standard method remains less accurate than the quadrupole method.

### 3.3. Advantages with respect to the standard method

The following is a short qualitative discussion of the three methods introduced above in relation to the properties of the background source galaxy populations.

Our starting point is the fact that the expected error on  $g$  depends on  $\sqrt{c}$ , i.e. it is larger for broader distributions. This has led us to introduce the weighted quadrupole method. On the other hand, the simple quadrupole method should also perform better than the standard method. This may be argued in the following way. Consider a simple case where all source galaxies are flat disks with the same luminosity and the same size. Then, for a random spatial orientation, all galaxies will appear as ellipses, with identical major axes and minor axes ranging from 0 to the size of the major axes. Therefore flatter source objects occupy smaller areas of the sky. In contrast with the standard method, the quadrupole method takes the galaxy size into account, which should lead to more accurate results. The argument can be extended to the case where different luminosities and sizes are involved. Furthermore, it should also be applicable to a more realistic galaxy population, since galaxy fields are usually dominated by spiral galaxies. This will be confirmed by our simulations (see Sect. 4).

It is also interesting to consider the case of a source population made of spheroids (i.e. axisymmetric ellipsoids). For a population of oblate galaxies we expect a behavior similar to that of disk galaxies. Thus if elliptical galaxies are generically oblate, their contribution would not alter the argument in favor of the quadrupole method. The situation is completely different for prolate spheroids, which behave in the opposite way; for a population dominated by prolate objects better results would be expected from application of the standard method.

Finally, it would be important to assess the error involved in the *measurement* of the ellipticity, but this would depend on a number of conditions characterizing the specific set of observations under investigation. Since the lensed galaxies are often smaller than  $1''$ , seeing can

be one important factor for ground observations. Seeing makes galaxies rounder and thus leads to an underestimate of the shear. Even if seeing effects can be partially resolved by means of special algorithms (such as maximum likelihood and maximum entropy image restoration; Lucy 1994), the error on the measured ellipticity should be larger for smaller galaxies. This is again in favor of the use of the quadrupole method, which downplays the role of small galaxies. For simplicity, seeing and other sources of error, such as Poisson noise, sky luminosity, and pixeling are not considered in this paper and in the simulations described below.

## 4. Monte Carlo simulations

### 4.1. Source galaxies

To test the various methods we have performed a series of Monte Carlo simulations of measurements of the reduced shear parameter  $g$ , by generating  $N$  galaxies as a realization of two types of source galaxies.

The first galaxy distribution (Population A) is characterized by a source ellipticity distribution inferred from about 6000 galaxies observed in a single frame obtained at the 200-inch Hale telescope at Palomar (Brainerd *et al.* 1996). Calling  $q$  the axis ratio of the galaxy (with  $0 \leq q \leq 1$ ), the empirical probability distribution for  $q$  is

$$p_q(q) \simeq 64q \exp(-8q). \quad (23)$$

The associated ellipticity distribution for  $\chi^s$  is shown in Fig. 1. The source galaxies are largely dominated by disk galaxies, with significant contributions from ellipticals. In order to specify the size distribution, for simplicity we have followed Wilson *et al.* (1996) in adopting exponential luminosity profiles for all the source objects, with scale-length  $h$  uniformly distributed in the range  $[0.25, 0.65]$  arcseconds. Finally, the position angle has been chosen randomly with uniform distribution. We have assumed that the three distributions (ellipticity, size, and position angle) are independent. A correlation between ellipticity and size might be present in a more realistic population of sources. Based on this choice of  $p_q(q)$  we have  $c \simeq 0.0606$ . Thus the expected error in the determination of  $g$  for both the standard method and the simple quadrupole method is  $\approx 0.015/N$ .

The second simple population of source galaxies (Population B) has been generated by assuming that all galaxies are flat disks of the same size and with random orientation (see also Bonnet & Mellier 1995). A straightforward calculation shows that the probability distribution for  $q$  is uniform, i.e.

$$p_q(q) = 1. \quad (24)$$

In this case we have  $c \simeq 0.2146$ . The associated distribution for  $\chi^s$  (see Fig. 1) shows a pronounced peak near

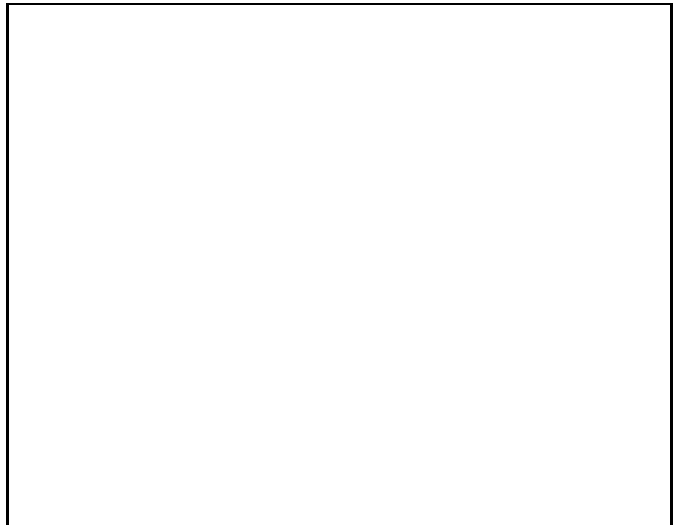


**Fig. 1.** The probability distribution of the source ellipticity for the two galaxy populations described in the text. The distribution is isotropic, i.e.,  $p(\chi^s) = p(|\chi^s|)$ .

$|\chi| = 1$ . This distribution is not sharp in the sense of Sect. 2.3, because of its relatively large value of  $c$ .

### 4.2. Simulations and results

The lens properties are then specified by means of the value of  $g_0$ ; the value of  $(1 - \sigma)$  does not affect the results. For a given lens, the observed quadrupole moment  $Q^{(n)}$  of each source is calculated by inverting Eq. (8)

$$Q^{(n)} = J^{-1} Q^{s(n)} J^{-1}. \quad (25)$$

From the set of observed quadrupole moments  $\{Q^{(n)}\}$  the methods X, Q, and W described in Sect. 2 and Sect. 3 allow us to determine the *measured* shear  $g$ . All methods involve the resolution of an implicit equation (Eq. (11), Eq. (14), and Eq. (21)); this has been done with a simple Newton-Raphson algorithm (see Press *et al.* 1992)

The entire process has been repeated a large number of times (typically 10,000), each time based on a different realization of the  $N$  source galaxies. Thus for each method, the mean of the measures of  $g$  and the related errors (covariance matrix) have been calculated. The simulations immediately provide a simple check on the mean of  $\chi^s$  and  $Q^s$  and on their covariance matrices, consistent with the relation  $c = b/M^2$  stated in Sect. 3.1. Then we have compared the average errors of each method with the expected error given by Eqs. (13) and (19). The main results for population A of galaxies are shown in Fig. 2, confirming the anticipated dependence on  $|g_0|$ ; the expected diagonal character of  $\text{Cov}_{ij}(g)$  for all the methods is also recovered.

As we can see from Fig. 3, the errors for the standard method (X) follow the  $1/\sqrt{N}$  law. They agree quite well



**Fig. 2.** The graphs show the mean error on  $g$  as a function of  $g_0$ . The error has been obtained from 10,000 simulations ( $N = 16$  galaxies, Pop. A) analyzed with the standard method (a), with the simple quadrupole method (b), and with the weighted quadrupole method (c). The results agree very well with the  $|1 - |g_0|^2|$  law.

with Eqs. (13) and (19) for all  $g_0$  values. From these results on the standard method, the galaxy distribution A is found to be sufficiently sharp. The error for the simple quadrupole method (Q) is instead about 15% lower than in the standard method for every value of  $g$  and  $N$  (see the short discussion given in Sect. 3.3). The weighted quadrupole method (W) shows even smaller errors: these are about 28% smaller than that of the standard method.

The results based on population B are qualitatively similar. The relevant ellipticity distribution is rather broad, and thus we expect Eq. (13) to give only approximate results. In fact, actual errors are about 30% larger

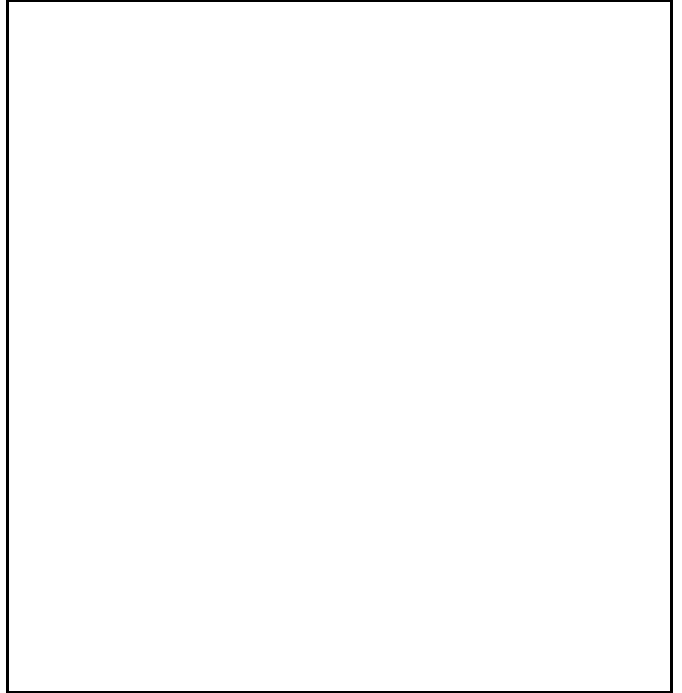


**Fig. 3.** The mean error on  $g$  versus the number  $N$  of galaxies used in the reconstruction process. Symbols are the results of the average error obtained with 10,000 simulations for the three specified methods, while the line is the  $1/\sqrt{N}$  law given by Eqs. (13) and (19). The value of  $g_0$  used is  $g_0 = 0.2 + 0.2i$ . The trends observed at  $N \sim 30$  have been checked to persist well beyond the range of  $N$  shown here.

than those stated in Eq. (13). For this galaxy population the differences among the three methods are more significant. The error in the simple quadrupole method is 27% smaller than that in the standard method, while in the weighted quadrupole method it is 38% smaller.

## 5. Impact on the mass measurement

The projected mass distribution  $\sigma(\boldsymbol{\theta})$  of a lens can be derived from a *map* of the reduced shear  $g$ , obtained by carrying out the procedure described above for many adjacent small patches of the sky. The analysis may be performed within a parameterised model for the lens. Here below we refer to the more general parameter-free approach.

The reconstruction of the lens mass distribution  $\sigma(\boldsymbol{\theta})$  from the map  $g(\boldsymbol{\theta})$ , with different ways of noise filtering, is based on the relation (see Seitz and Schneider 1996)

$$\begin{aligned} \nabla S(\boldsymbol{\theta}) &= \frac{1}{1 - |g|^2} \begin{pmatrix} 1 + g_1 & g_2 \\ g_2 & 1 - g_1 \end{pmatrix} \begin{pmatrix} g_{1,1} + g_{2,2} \\ g_{2,1} - g_{1,2} \end{pmatrix} \\ &\equiv \mathbf{u}(\boldsymbol{\theta}), \end{aligned} \quad (26)$$

where  $S(\boldsymbol{\theta}) = \ln(1 - \sigma(\boldsymbol{\theta}))$ . Here  $g_{i,j}$  indicates the partial derivative of  $g_i$  with respect to  $\theta_j$ . Equation (26) shows that, if  $g$  is known, one can determine  $(1 - \sigma)$  only up

to a multiplicative constant. In general, the reconstructed mass is given in the form

$$S(\boldsymbol{\theta}) - S_0 = \int \mathbf{K}(\boldsymbol{\theta}, \boldsymbol{\theta}') \cdot \mathbf{u}(\boldsymbol{\theta}') d^2\boldsymbol{\theta}', \quad (27)$$

where  $\mathbf{K}(\boldsymbol{\theta}, \boldsymbol{\theta}')$  is a suitable kernel. The integration is performed over the observation area. In Sect. 4.2 the weighted quadrupole method has been shown to lead to errors in the determination of  $g$  that are significantly smaller than those of the standard method. This in turn implies smaller errors on the reconstructed mass distribution  $\sigma(\boldsymbol{\theta})$ . In fact, in the sharp distribution limit the covariance matrix of every derived variable is directly proportional to the covariance matrix of the original variable. This in practice suggests that the weighted quadrupole method should lead to a covariance of  $\sigma(\boldsymbol{\theta})$  smaller by a factor of  $\approx 30\%$  with respect to the standard method. Similarly, one could argue that the error on the total mass is expected to be reduced by the same factor. Of course, this is only a quick estimate. We have considered the full problem in detail, but here we leave out the related calculations, since this analysis would bring us well beyond the scope of the present paper.

## 6. Conclusions

In this paper we have analyzed in detail different methods aimed at obtaining the reduced shear  $g$  from the observed ellipticities of a set of galaxies and we have focused on the issue of the accuracy of such measurement. Monte Carlo simulations have demonstrated that realistic distributions in general favor a new method introduced in this paper, called the quadrupole method. In particular, the weighted quadrupole method has been shown to perform best (the gain is of the order of  $\approx 15\text{--}30\%$  for the simple quadrupole method and of the order of  $\approx 30\text{--}40\%$  for the weighted quadrupole method). This in turn leads to more accurate mass determinations.

*Acknowledgements.* We thank Peter Schneider for helpful discussions and suggestions on the subject. This work has been partially supported by MURST of Italy.

## Appendix A: The expected covariance matrix for a sharp ellipticity distribution

In order to calculate the covariance expected in a measurement of  $g$  with the methods described in the main text, we use a general expression known in the theory of errors (see Taylor 1982). Let  $X$  be a multidimensional random variable and let  $Y = f(X)$ . Suppose that  $f$  is a smooth function and that the probability distribution of  $X$  is sharp, so that its covariance matrix  $\text{Cov}(X)$  is

small. Then we have (basically this is an application of the saddle-point integration method)

$$\langle Y \rangle \simeq f(\langle X \rangle), \quad (A1)$$

$$\text{Cov}(Y) \simeq C \text{Cov}(X) C^T. \quad (A2)$$

Here  $C$  is the Jacobian matrix for  $f$  calculated for the mean value of  $X$ , i.e.

$$C = \left. \frac{\partial f}{\partial X} \right|_{X=\langle X \rangle}. \quad (A3)$$

If  $Y$  is implicitly defined by  $F(X, Y) = 0$ , we can equally well apply the previous relations using the inverse function theorem. In this case the mean value of  $Y$  is implicitly provided by  $F(\langle X \rangle, \langle Y \rangle) = 0$ , while  $C = -B^{-1}A$  with

$$A = \left. \frac{\partial F}{\partial X} \right|_{X=\langle X \rangle, Y=\langle Y \rangle}, \quad (A4)$$

$$B = \left. \frac{\partial F}{\partial Y} \right|_{X=\langle X \rangle, Y=\langle Y \rangle}. \quad (A5)$$

In conclusion in this case we have

$$F(\langle X \rangle, \langle Y \rangle) \simeq 0, \quad (A6)$$

$$\text{Cov}(Y) \simeq (B^{-1}A) \text{Cov}(X) (B^{-1}A)^T. \quad (A7)$$

Based on these expressions we can easily prove Eqs. (12, 13) for the standard method, and (18, 19) for the simple quadrupole method.

### A.1. Standard method

In the standard method the reduced shear  $g$  is calculated from Eq. (11). In principle this equation depends on  $N$  complex random variables  $\chi^{(n)}$  and on the unknown reduced shear  $g$ . The expected average for the observed ellipticity  $\chi$  is easily obtained from the inverse of Eq. (9), that is

$$\chi = \frac{\chi^s - 2g + \chi^{s*} g^2}{1 - 2\text{Re}(\chi^{s*} g) + |g|^2}. \quad (A8)$$

By setting  $\chi^s = \langle \chi^s \rangle = 0$ , this gives the mean

$$\langle \chi \rangle = -\frac{2g_0}{1 + |g_0|^2}. \quad (A9)$$

As in the main text,  $g_0$  represents the *real* value of  $g$ . Note that this equation could be used to determine  $g_0$  in a simple way from a measurement of the observed mean of  $\chi$ .

The expected mean of measurements of  $g$  obtained from Eq. (11) obeys the relation

$$\frac{1}{N} \sum_{n=1}^N \chi^s(\langle \chi \rangle, \langle g \rangle) = 0. \quad (A10)$$

Using the calculated mean  $\langle \chi \rangle$  of Eq. (A9) above we thus prove Eq. (12).

Following Eq. (A7), the covariance matrix for  $g$  can be written as

$$\text{Cov}(g) = \frac{1}{N} (B^{-1}A) \text{Cov}(\chi) (B^{-1}A)^T. \quad (\text{A11})$$

The two matrices  $A$  and  $B$  are the partial derivatives of  $\chi^s(\chi, g)$ :

$$A = \left. \frac{\partial \chi^s(\chi, g)}{\partial \chi} \right|_{\chi=\langle \chi \rangle, g=\langle g \rangle}, \quad (\text{A12})$$

$$B = \left. \frac{\partial \chi^s(\chi, g)}{\partial g} \right|_{\chi=\langle \chi \rangle, g=\langle g \rangle}. \quad (\text{A13})$$

The covariance matrix  $\text{Cov}(\chi)$  can be expressed, by application of the inverse function theorem, as

$$\text{Cov}(\chi) = A^{-1} \text{Cov}(\chi^s) (A^{-1})^T = cA^{-1} (A^{-1})^T, \quad (\text{A14})$$

so that Eq. (A11) becomes

$$\text{Cov}(g) = \frac{c}{N} B^{-1} (B^{-1})^T. \quad (\text{A15})$$

A simple algebraic calculation leads to

$$B = \frac{2}{1 - |g_0|^2} \text{Id} \quad (\text{A16})$$

and thus we recover Eq. (13).

### A.2. Simple quadrupole method

To show that the simple quadrupole method leads to similar results, we start by considering the expected distribution for the observed quadrupoles  $Q$ . From Eq. (16) in the sharp distribution limit we have

$$\langle Q \rangle = MJ^{-2}. \quad (\text{A17})$$

Here  $J^{-2}$  indicates  $(J^{-1})^2$ , i.e. the square of the inverse matrix of  $J$ . The expected average of  $g$  is calculated by solving Eq. (14) with  $g$  replaced by  $\langle g \rangle$ , i.e.

$$\chi^s(\langle Q \rangle, \langle g \rangle) = 0. \quad (\text{A18})$$

Since  $\chi^s(Q, g) \equiv \chi(JQJ)$ , with  $J$  any matrix with associated reduced shear equal to  $g$ , we recover Eq. (18).

In order to calculate the covariance matrix of  $g$ , we use Eq. (A7). From Eq. (A2), the covariance of  $Q$  (recall the definition  $Q_{ij} = Q_{i+j-1}$ ) can be written as

$$\text{Cov}(Q) = C \text{Cov}(Q^s) C^T, \quad (\text{A19})$$

where  $C$  is the Jacobian matrix

$$C = \left. \frac{\partial Q(Q^s, g)}{\partial Q^s} \right|_{Q^s=\langle Q^s \rangle, g=\langle g \rangle}. \quad (\text{A20})$$

In the quadrupole method, the matrices  $A$  and  $B$  of Eqs. (A4) and (A5) are given by

$$A = \left. \frac{\partial \chi^s(Q^s, g)}{\partial Q} \right|_{Q=\langle Q \rangle, g=\langle g \rangle}, \quad (\text{A21})$$

$$B = \left. \frac{\partial \chi^s(Q^s, g)}{\partial g} \right|_{Q=\langle Q \rangle, g=\langle g \rangle}, \quad (\text{A22})$$

where the average values of  $Q$  and  $g$  are stated in Eqs. (A17) and (18). Note that the matrix  $B$  defined here is the same as the one used for the standard method and defined in Eq. (A13). The covariance matrix for  $g$  is then

$$\begin{aligned} \text{Cov}(g) &= (B^{-1}A) \text{Cov} \left( \frac{1}{N} \sum_{n=1}^N Q^{(n)} \right) (B^{-1}A)^T \\ &= \frac{1}{N} (B^{-1}A) C \text{Cov}(Q^s) C^T (B^{-1}A)^T. \end{aligned} \quad (\text{A23})$$

Therefore we have

$$AC = \left. \frac{\partial \chi^s}{\partial Q} \frac{\partial Q}{\partial Q^s} \right|_{Q^s=\langle Q^s \rangle} = \left. \frac{\partial \chi^s}{\partial Q^s} \right|_{Q^s=\langle Q^s \rangle} \quad (\text{A24})$$

and thus

$$ACC\text{Cov}(Q^s)(AC)^T = \text{Cov}(\chi^s) = c \text{Id}. \quad (\text{A25})$$

Using Eq. (A16) we finally obtain Eq. (19).

### A.3. The dependence on $g$

From local observations it is not possible to choose between two different solutions for the reduced shear related by  $g' = 1/g^*$ . We thus expect that the expression for the error will incorporate this invariance property.

The  $g \mapsto 1/g^*$  transformation is equivalent to a change of sign in one eigenvalue of  $J$  (see Schneider & Seitz 1995a), which is not observable. Every reconstruction method is then bound to give two solutions for the reduced shear. As  $g'$  is related to  $g$ , we can calculate the expected error on  $g'$  given the error on  $g$ :

$$\text{Cov}(g') = \left( \frac{\partial g'}{\partial g} \right) \text{Cov}(g) \left( \frac{\partial g'}{\partial g} \right)^T.$$

A simple calculation gives

$$\left( \frac{\partial g'}{\partial g} \right) = \frac{1}{|g|^4} \begin{pmatrix} g_1^2 - g_2^2 & -2g_1g_2 \\ -2g_1g_2 & g_2^2 - g_1^2 \end{pmatrix} \quad (\text{A26})$$

so that, as  $\text{Cov}(g) \propto \text{Id}$ , we have

$$\begin{aligned} \text{Cov}(g') &= \frac{1}{|g|^4} \text{Cov}(g) = \frac{c(1/|g|^2 - 1)^2}{4N} \text{Id} \\ &= \frac{c(1 - |g'|^2)^2}{4N} \text{Id}. \end{aligned} \quad (\text{A27})$$

Hence our expression for the error on  $g$  reflects the  $g \mapsto 1/g^*$  invariance.

## Appendix B: Basic structure of the simulation algorithm

The simulation algorithm, briefly described in Sect. 4, is composed of three different parts.

For a given galaxy distribution, we have generated  $N$  source galaxies (quadrupoles) using the rejection method (see Press *et al.* 1992). Then we have calculated, using Eq. (25), the observed quadrupoles and ellipticities.

Different methods (X, Q, and W) have been applied by solving respectively Eqs. (11), (14), and (21) with a simple Newton-Raphson algorithm. This algorithm requires an initial point for the unknown  $g$ . This has been chosen using Eq. (A9). Through the entire simulation algorithm we have supposed to be able to distinguish between the two solutions  $g$  and  $1/g^*$ . In practical cases this is easy if the lens is non-critical. For critical lenses this ambiguity can be resolved only globally. Note that this assumption has been implicitly made throughout the paper (e.g., consider the justification of Eqs. (A10) and (A18)).

The previous steps have been repeated a large number of times with the same  $g_0$ . For each individual “simulation” we have memorized the calculated value of  $g$ . Finally, the mean and the covariance matrix have been calculated from the data base of all the available results.

The algorithm has been implemented as a C++ code running on a IBM RISC System/6000 590 machine.

## References

Bonnet H., Mellier Y., 1995, A&A 303, 331

- Brainerd T.G., Blandford R.D., Smail I., 1996, ApJ 466, 623
- Gould, A., Villumsen, J., 1994, ApJ 428, 45
- Griffiths R.E., Casertano S., Im M., Ratnatunga K.U., 1996, MNRAS 282, 1159
- Kaiser N., Squires G., 1993, ApJ 404, 441
- Kaiser N., Squires G., Broadhurst T., 1995, ApJ 449, 460
- Kneib J.B., Soucail G., 1995, in: “Astrophysical applications of gravitational lensing”, Proc. IAU Symp. 173, ed. C.S. Kochanek & J.N. Hewitt, Kluwer, Dordrecht, p. 129
- Kneib J.B., Ellis R.S., Smail I., Couch W.J., Sharples R.M., 1996, ApJ 471, 643.
- Lucy L.B., 1994, A&A, **289**, 983
- Press W.H., Teukolsky S.A., Vetterling W.T., Flannery B.P., 1992 Numerical Recipes in C, Cambridge University Press, Cambridge
- Schneider P., Ehlers J., Falco E.E., 1992, Gravitational Lenses, Springer, Heidelberg
- Schneider P., Seitz C., 1995a, A&A 294, 411
- Schneider P., Seitz C., 1995b, A&A 297, 287
- Seitz S., Schneider P., 1996, A&A 305, 383
- Taylor, J.R. 1982, An Introduction to Error Analysis: The Study of Uncertainties in Physical Measurements, University Science Books
- Tyson J.A., Valdes F., Jarvis J.F., Mills A.P., 1984, ApJ 281, L59
- Webster R.L., 1985, MNRAS 213, 871
- Wilson G., Cole S., Frenk C.S., 1996, MNRAS 280, 199

special character #1: Cov

This article was processed by the author using Springer-Verlag  $\text{\TeX}$  A&A macro package 1992.

